# Identification of immunogenic cell death-related prognostic signatures in pancreatic cancer

WENJING YU, MEI LI and JING XIA

Department of Laboratory Medicine, The 13th People's Hospital of Chongqing, Chongqing 400053, P.R. China

Received December 12, 2022; Accepted August 22, 2023

DOI: 10.3892/ol.2023.14061

**Abstract.** Targeting immunogenic cell death (ICD) may enable the response of pancreatic cancer to immune checkpoint inhibitors (ICIs). The aim of the present study was to elucidate the role of ICD-related genes in pancreatic cancer. Utilizing the k-means method, consensus clustering was employed to effectively group patients with pancreatic cancer. Subsequently, a set of differentially expressed genes was identified between the two subtypes related to ICD, facilitating the execution of a comprehensive enrichment analysis. Furthermore, the construction of an ICD-related prognostic signature (IRPS) was accomplished through LASSO Cox regression, thereby enabling the assessment of responses to both chemotherapy and immunotherapy. In addition, the biological functionality of 5'-nucleotidase ecto (NT5E) was elucidated through experimental investigations. Patients characterized as the ICD high subtype experienced a comparatively shorter overall survival. This subtype exhibited a noteworthy correlation with HLA families and immune checkpoint molecules, underscoring its immunological significance. Subsequently, patients with elevated IRPS risk scores displayed resistance towards immunotherapy interventions. Of note, synergistic downregulation of NT5E in combination with Gemcitabine was observed to significantly induce tumor cell apoptosis, emphasizing its potential therapeutic value. Leveraging ICD-related genes, a novel classification system was meticulously devised to comprehensively evaluate both the clinical outcomes and therapeutic responses of patients diagnosed with pancreatic cancer.

*Correspondence to:* Dr Jing Xia, Department of Laboratory Medicine, The 13th People's Hospital of Chongqing, 16 Tielu New Village, Jiulongpo, Chongqing 400053, P.R. China
E-mail: xiajingcq007@163.com

*Abbreviations:* ICD, immunogenic cell death; DAMPs, damage-associated molecular patterns; TME, tumor microenvironment; ICI, immune checkpoint inhibitor; DEG, differentially expressed gene; IRPS, ICD-related prognostic signature; OS, overall survival; HMGB1, high mobility group box protein B1; IFN I, type I interferon; APCs, antigen-presenting cells; TCGA, The Cancer Genome Atlas; GO, Gene Ontology; LASSO, Least Absolute Shrinkage and Selection Operator; PFS, progression-free survival; ROC, receiver operating characteristic; TMB, tumor mutation burden; TIDE, Tumor Immune Dysfunction and Exclusion; FBS, fetal bovine serum

*Key words:* immunogenic cell death, pancreatic cancer, tumor immune microenvironment, immune checkpoint inhibitor, TCGA

## Introduction

Pancreatic cancer remains closely correlated with an unfavorable prognosis, characterized by a 5-year overall survival (OS) rate of <5% (1). Despite the implementation of surgical resection coupled with chemoradiotherapy, the 5-year OS rate was only marginally improved to 20-25% (2). Of note, a paradigm shift in pancreatic cancer treatment has emerged with the advent of immune checkpoint molecule targeting (3). Immune checkpoint inhibitors (ICIs) have the ability to activate T cells, offering a promising avenue for tumor immunotherapy. Examples include anti-cytotoxic T-lymphocyte-associated protein 4 and anti-programmed cell death 1 agents (4). In essence, the identification of biomarkers capable of serving as targets for immunotherapy, while also predicting both the prognosis of patients with pancreatic cancer and their responsiveness to chemotherapy, holds immense potential. Such biomarkers may substantially enhance treatment effectiveness and simultaneously mitigate unnecessary interventions in the realm of pancreatic cancer therapy (5).

Immunogenic cell death (ICD) represents a regulated form of cell demise triggered by treatments such as chemotherapy and radiotherapy. This process effectively prompts an immune response within the tumor microenvironment (TME) (6). ICD achieves this by liberating tumor-associated antigens and tumor-specific antigens, thereby setting off critical 'danger signals' that serve as triggers for immune activation (7). Of note, ICD is characterized by the release and elevation of damage-related molecular patterns (DAMPs), pro-antigen inflammatory cytokines and inflammatory mediators. Among the DAMPs, significant players encompass ATP, calreticulin, high mobility group box protein B1 (HMGB1), heat shock proteins, type I interferon (IFN) and Annexin 1. The orchestration of these molecules culminates in the activation and recruitment of antigen-presenting cells, subsequently prompting T-cell activation and an adaptive immune response directed at tumor antigens. Recognizing the potential of combining multiple immunotherapeutic strategies

rooted in ICD induction, a novel avenue for advancing tumor immunotherapy emerges, exemplified by the synergy achieved through combined ICIs (8). Consequently, the exploration of therapeutic targets and methodologies associated with ICD holds a prominent position in contemporary pancreatic cancer research.

In the present study, a comprehensive analysis was conducted involving consensus clustering of pancreatic cancer samples into two distinct subtypes based on the expression patterns of ICD-associated genes (Fig. 1). Of note, high ICD levels were found to be associated with unfavorable prognostic outcomes and compromised immune status in patients with pancreatic cancer. Furthermore, an innovative prognostic signature named the ICD-Related Prognostic Signature (IRPS) was devised and its efficacy in predicting individual responses to both chemotherapy and immunotherapy interventions was demonstrated. The present results shed new light on the potential immunotherapeutic strategies to manage pancreatic cancer.

## Materials and methods

*Patient data acquisition*. Gene expression data, alongside clinical data and single nucleotide mutation data of 183 patients with pancreatic cancer were obtained from The Cancer Genome Atlas (TCGA) data portal (https://cancergenome.nih.gov/). Subsequent to the exclusion of cases with incomplete clinical information (included survival status or time, T, N, and M stage), a comprehensive follow-up dataset comprising 175 patients was compiled for analysis (female, n=78; male, n=97; age, >60 years, n=119; age ≤60 years, n=56). The dataset GSE183795 (9), containing 105 samples of normal pancreatic tissue and 139 samples of pancreatic cancer tissue, was downloaded from the Gene Expression Omnibus (GEO) database (https://www.ncbi.nlm.nih.gov/geo/).

*Consensus clustering*. A collection of 34 ICD-related genes, as delineated in previous studies (10,11), was curated. Protein-protein interaction network was visulized by STRING (https://cn.string-db.org/). These genes were subsequently subjected to a consensus clustering analysis through the utilization of the 'ConsensusClusterPlus' package of the R software. The K-means clustering algorithm was employed to discern and delineate robust and stable ICD-related subtypes within the realm of pancreatic cancer.

*Functional enrichment analysis*. The 'Limma' package of R software was used for the identification of differentially expressed genes (DEGs), with a screening threshold set at a false discovery rate-corrected P<0.001 and |log fold change| >2. Subsequently, these DEGs underwent comprehensive functional elucidation and pathway analysis through the application of Gene Ontology (GO) and Kyoto Encyclopedia of Genes and Genomes (KEGG). The enrichment analyses for GO and KEGG were conducted using the 'clusterProfiler' package.

*Association between ICD-related subtypes and somatic mutations or TME*. For the visualization of copy number variation (CNV) data, the 'ComplexHeatmap' package of the R software was employed to generate a waterfall plot. The composition of 22 immune-infiltrating cell types was quantified using the CIBERSORT methodology. Furthermore, the ESTIMATE algorithm was applied to calculate both stromal scores and immune scores. To discern distinctions between the two ICD subtypes, a comparison of the expression levels of human leukocyte antigen (HLA) gene families and immune checkpoint molecules was undertaken.

*Construction of the IRPS*. ICD-related genes were utilized to perform univariate Cox regression analysis and subsequent Least Absolute Shrinkage and Selection Operator Cox regression analysis to calculate coefficient values. The risk score for each patient was calculated according to the following formula: Risk score=$\sum_{k=0}^{n} coef(k) * x(k)$, where coef (k) and x (k) are regresion coefficients. The OS or progression-free survival (PFS) and the receiver operating characteristic (ROC) curve were used to determine the prognostic value of the IRPS.

*Relationship between IRPS model and TME or response to immunotherapy*. The tumor mutation burden (TMB) was quantified by tallying the number of mutations within each sample. Leveraging the R package 'pRRophetic' of the R software, an exploration was conducted to pinpoint potential drugs with sensitivity for pancreatic cancer, guided by the ICD-related prognostic signature. To gauge the anticipated response to immunotherapy, Tumor Immune Dysfunction and Exclusion (TIDE; http://tide.dfci.harvard.edu/) was applied.

*Human Protein Atlas*. Immunohistochemical staining images of caspase 1 (CASP1) [Tumor (n=23), Normal (n=3)] and 5'-nucleotidase ecto (NT5E) [Tumor (n=46), Normal (n=6)] in normal and pancreatic cancer tissues (poor differentiation; moderate differentiation; highly differentiation) were obtained from the Human Protein Atlas (https://www.proteinatlas.org/). The staining intensity was scored as follows: None, 0; pale yellow, 1; brownish yellow, 2; deep brown, 3. The percentage of positive staining was scored as follows: 0-5%, 0; 6-25%, 1; 26-50%, 2; 51-75%, 3; >75%, 4. For scoring a certain type of cells, 5 fields of view were selected and 100 cells of this type per 400x high-magnification field were counted. The formula for the final staining score was as follows: Staining intensity per field of view x Positive cell percentage. The rating was as follows: 0 points, negative; 1-4 points, weakly positive; 5-8 points, moderately positive; 9-12 points, strongly positive.

*Cell culture*. The human pancreatic cancer cell lines ASPC-1, PANC-1, SW1990 and T3M4 and the normal ductal epithelial cell line hTERT-HPNE were obtained from the American Type Culture Collection. Pancreatic cancer cells were cultured in DMEM (Gibco; Thermo Fisher Scientific, Inc.) + 10% fetal bovine serum (FBS; Gibco; Thermo Fisher Scientific, Inc.) in a cell incubator with 5% $CO_2$ at 37˚C. hTERT-HPNE cells were cultured in DMEM with 1 ng/ml epidermal growth factor (cat. no. HY-P7109; MedChemExpress) and 10% FBS.

*Western blot analysis*. Extracted cells were suspended in cell lysis buffer (cat. no. P0013; Beyotime Institute of Biotechnology). The protein concentration in each group was determined using a BCA protein assay kit (cat. no. P0012S; Beyotime Institute of Biotechnology). Roughly 40 $\mu$g of denatured protein was

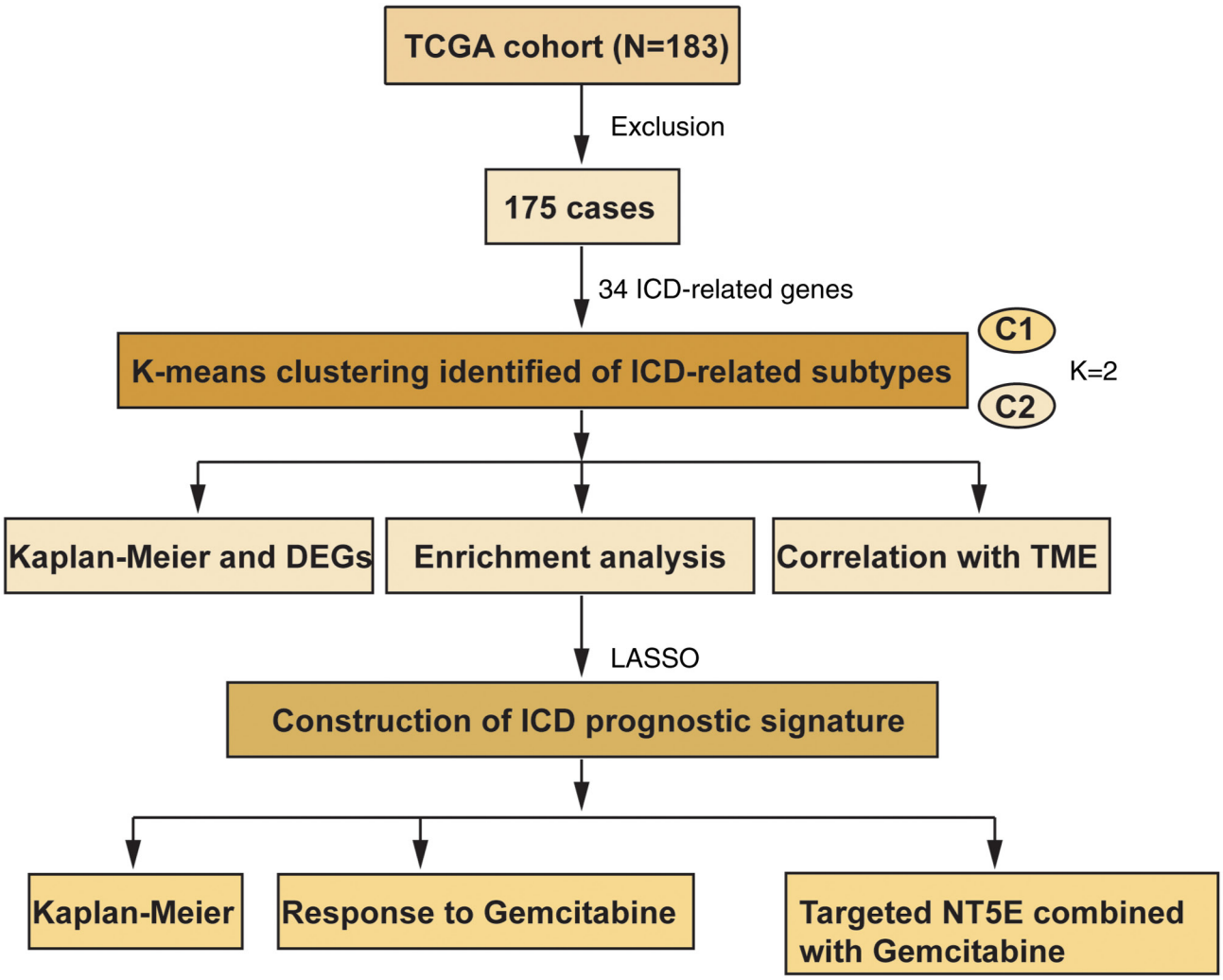


Figure 1. Flow chart of the present study. TCGA, The Cancer Genome Atlas; DEG, differentially expressed gene; TME, tumor microenvironment; ICD, immunogenic cell death; NT5E, 5'-nucleotidase ecto; LASSO, Least Absolute Shrinkage and Selection Operator.

loaded into 10% SDS-PAGE gels and subjected to electrophoresis at 200V. Subsequently, the proteins were transferred to a PVDF membrane (Merck Millipore), followed by blocking with 5% skimmed milk for 1 h at 37˚C. The PVDF membrane was then subjected to an overnight incubation at 4˚C with the following primary antibodies: Anti-NT5E (cat. no. ab133582), anti-Bcl-2 (cat. no. ab32124), anti-Bax (cat. no. ab32503) and anti-β-actin (cat. no. ab8226; all from Abcam; 1:1,000 dilution). On the following day, the PVDF membrane was exposed to secondary antibody [anti-rabbit (cat. no. 7074) or anti-mouse IgG (cat. no. 7076); both from Cell Signaling Technology, Inc.; 1:2,000 dilution] for 1 h at room temperaure. Chemiluminescent substrate (cat. no. WBKLS0500; Merck KGaA) was applied according to the manufacturer's protocol, and chemiluminescence was captured using a Molecular Imager ChemiDoc XRS+ (Bio-Rad Laboratories, Inc.). Image Lab software v5.0 (Bio-Rad Laboratories, Inc.) was employed for subsequent analysis.

*Reverse transcription-quantitative (RT-q)PCR*. RNAiso Plus Regent (Takara Bio, Inc.) was used to extract total RNA from harvested cells. RNA was reverse transcribed to cDNA using a High Capacity cDNA kit (cat. no. 4374966; Applied Biosystems; Thermo Fisher Scientific, Inc.) according to the manufacturer's protocol. Real-time qPCR was performed with TB GREEN (Takara Bio, Inc.) according to the manufacturer's protocol using an ABI Prism 7900HT Sequence Detection System (Applied Biosystems; Thermo Fisher Scientific, Inc.). The thermocycling conditions were as follows: Initial denaturation at 95˚C for 30 sec, followed by 40 cycles of denaturation, annealing, elongation (95˚C for 20 sec, 55˚C for 20 sec and 72˚C for 20 sec, respectively), and final extension (95˚C for 10 sec). The primer sequences were as follows: GAPDH sense, 5'-GCACCGTCAAGGCTGAGAAC-3' and antisense, 5'-ATGAGGTCCACCACCCTGTTG-3'; NT5E sense, 5'-AGCGAGGACTCCAGCAAGTG-3' and antisense, 5'-CTTGATCCGACCTTCAACTGCTG-3'. GAPDH was used as an internal reference, and relative mRNA expression was calculated using the $2^{-\Delta\Delta Cq}$ method (12).

*Lentiviral transfection*. Lentiviruses [short hairpin RNA (sh)-NT5E and negative control] were purchased from Shanghai GenePharma Co., Ltd. The sequences were as follows: sh-NT5E, 5'-GGATACACTTCCAAAGAAA-3'; negative control, 5'-GATGGAGAAGCTCGCTGATTT-3'. The pancreatic cancer cells were transfected with lentivirus

according to the manufacturer's instructions and the stably transfected cells were selected by puromycin (2 $\mu$g/ml; cat. no. A1113803; Thermo Fisher Scientific, Inc.) for two weeks. Extraction of total protein and detection of knockdown efficiency were then performed.

*Cell viability assay*. Roughly $1x10^4$ cells were plated per well in 96-well plates and allowed to incubate for 24 h. Following treatment with Gemcitabine (1 $\mu$M; cat. no. HY-B0003; MedChemExpress), the cell viability was determined by treating the cells with CCK-8 reagent (cat. no. 96992-3000TESTS-F; Merck KGaA) at 37˚C for 2 h, in accordance with the manufacturer's instructions. Subsequently, the absorbance was recorded at 564 nm using a microplate reader (Infinite 200 PRO; Tecan Group, Ltd.) to quantify cell viability.

*Apoptosis assessment*. Approximately $1x10^6$ cells originating from each group were subjected to incubation with Annexin V-FITC (20 $\mu$g/ml) and propidium iodide (50 $\mu$g/ml; cat. no. C1062M; Beyotime Institute of Biotechnology) for a duration of 30 min. Subsequent to incubation, flow cytometry using FC500 (Beckman Coulter, Inc.) was employed to determine cell apoptosis, and data were then subjected to analysis using BD CellQuest Pro (v 5.1; BD Biosciences).

*Statistical analysis*. Values are expressed as the mean ± standard deviation. R software (v.4.2.1) and SPSS (v.19.0; IBM Corp.) were used to perform analysis and visualization. Spearman correlation analysis was used to determine the correlation between immune cells. Kaplan-Meier plotter (https://kmplot.com) was used for survival analysis. DComparisons of two groups were performed by unpaired Student's t-tests. One-way ANOVA was used to conduct comparisons of multiple groups, followed by Tukey's post-hoc test. $P<0.05$ was considered to indicate statistical significance.

## Results

*Identification of two ICD-related subtypes*. Utilizing a set of 34 ICD-related genes, a consensus clustering analysis was conducted on pancreatic cancer samples. Of note, certain ICD-related genes exhibited abnormal expression in pancreatic cancer samples from the TCGA and GSE183795 datasets (Fig. 2A and B). The protein-protein interaction network of these downregulated genes was further visualized using the STRING database (Fig. S1). Moving forward, a consensus clustering analysis was performed, yielding the grouping of pancreatic cancer samples into two distinct subtypes through the application of the K-means algorithm (Fig. 2C). Of note, the ICD-related genes displayed an upregulation trend within cluster C1, corresponding to the ICD-high subtype (Fig. 2D). In addition, the OS of patients in the ICD-high group was significantly shorter (Fig. 2E). Collectively, these findings underscore the prognostic significance of ICD-related genes within the context of pancreatic cancer.

*Identification of DEGs between ICD subtypes*. Subsequently, leveraging the prognostic significance attributed to ICD-related genes, identification of DEGs was performed for subsequent enrichment analysis. The DEGs were visually represented through both heatmap and volcano plot depictions (Fig. 3A and B). As presented in Figs. 2B and 3B, cluster 2 or downregulated genes were so few that enrichment analysis could not be performed. Accordingly, the current enrichment analysis primarily represents the enrichment results of upregulated genes or cluster 1. Of note, GO enrichment analysis indicated that DEGs exhibited enrichment in various immune-related functions, encompassing processes such as 'immunoglobulin production', 'production of molecular mediator of immune response', 'antigen binding', 'T-cell receptor complex' and 'B-cell receptor signaling pathway' (Fig. 3C and D). Furthermore, KEGG enrichment analysis highlighted the involvement of the DEGs with immune-related pathways, including 'cytokine-cytokine receptor interaction', 'focal adhesion', 'ECM-receptor interaction' and 'PI3K-AKT signaling pathway' (Fig. 3E). These results emphasize the substantial involvement of the DEGs in various immune processes, ultimately shedding light on their roles within the realm of immunity.

*ICD-related subtypes are associated with TME and mutations*. To shed light on the connection between somatic mutations and ICD-related subtypes, the somatic mutation profiles within the two subtypes were visualized. Of note, the ICD-high subtype exhibited a higher frequency of somatic mutations (Fig. 4A and B). These mutations included KRAS (67%), TP53 (63%), SMAD4 (24%), CDKN2A (19%) and TTN (12%), among others. Moving forward, a comparative analysis of TME composition revealed that the ICD-high subtype displayed elevated values in terms of the estimate score, immune score and stromal score (Fig. 4C-E). Conversely, the ICD-low subtype exhibited lower tumor purity (Fig. 4F).

Further exploration encompassed the assessment of immune cell infiltration between two subtypes. Utilizing CIBERSORT, the composition of 22 distinct immune cell types within the 175 pancreatic cancer samples was visualized (Fig. 4G). Of note, a positive correlation was observed between CD4-naive T cells and CD4 memory-activated T cells, while macrophages M0 demonstrated a negative correlation with T cells CD8 (Fig. 5A). Specifically, the fraction of T cells gamma delta was noted to be upregulated among patients in the ICD high group (Fig. 5B). Furthermore, a substantial portion of HLA gene families and immune checkpoint molecules displayed upregulation in the ICD-high group (Fig. 5C and D). These collective findings firmly establish the association between ICD-related subtypes and the intricate status of the tumor immune milieu.

*Construction of IRPS model*. Subsequently, the ICD-related genes were harnessed to construct a prognostic signature. Employing univariate Cox regression analysis, nine ICD-related genes were identified that exhibited associations with OS (Fig. 6A). Out of these, two ICD-related genes were meticulously chosen for the construction of the IRPS model (Fig. 6B and C). The OS and PFS of individuals categorized as high-risk were notably shorter in comparison to those classified as low-risk (Fig. 6D and E). This trend was mirrored in the higher count of deceased patients within the high-risk group (Fig. 7A). Both univariate and multivariate Cox

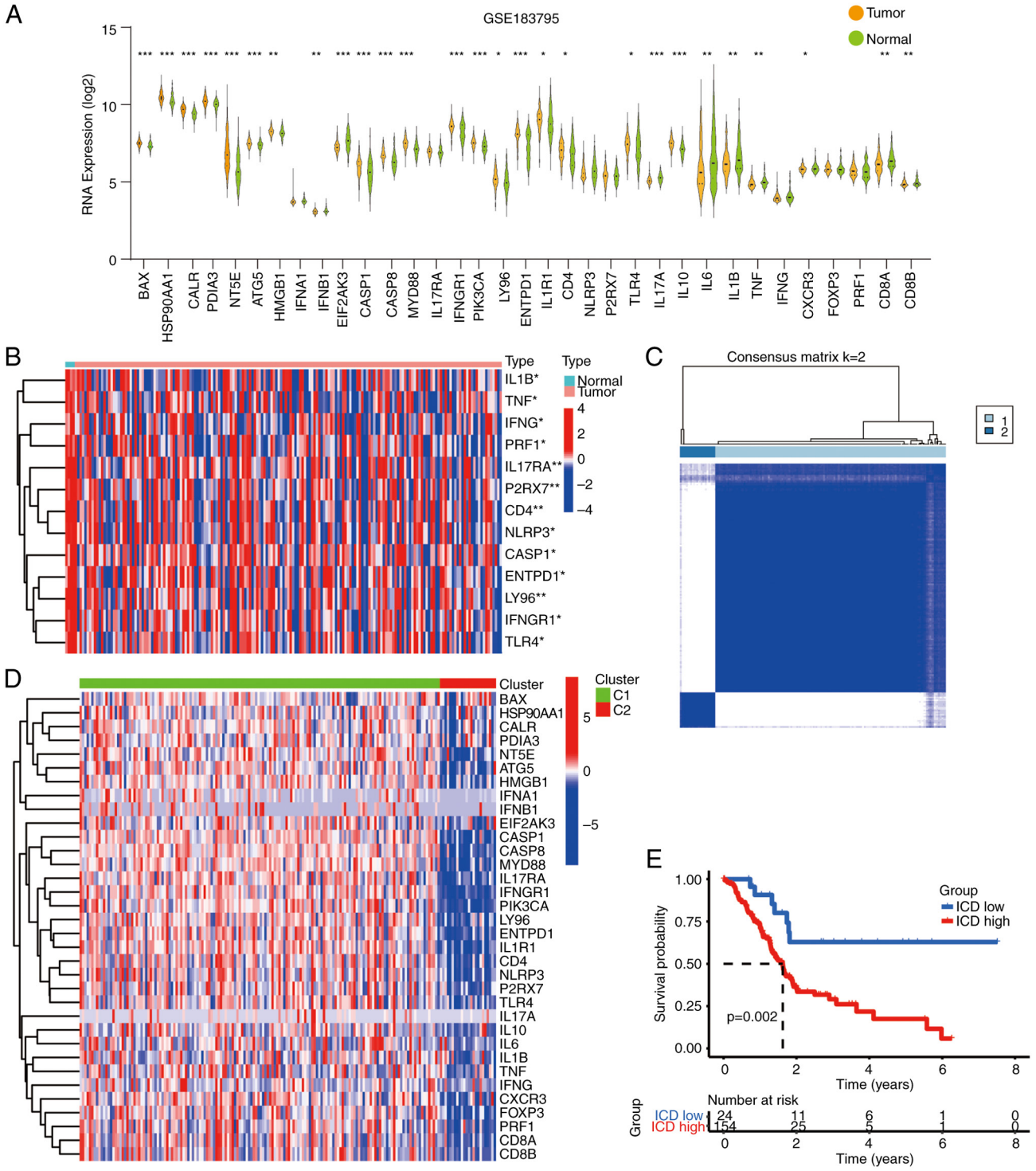


Figure 2. Clustering analysis of differential gene expression in pancreatic cancer. (A) Differentially expressed ICD-related genes in pancreatic cancer. (B) Heatmap of differentially expressed genes in pancreatic cancer and normal samples. (C) ICD-related genes were upregulated in pancreatic cancer. 1, cluster 1; 2, cluster 2. (D) Heatmap of differentially expressed genes in cluster 1 and 2. (E) Kaplan-Meier analysis indicated that patients in the ICD high group had poor prognosis. $^{*}$P<0.05, $^{**}$P<0.01, $^{***}$P<0.001. ICD, immunogenic cell death.

regression analyses demonstrated that the IRPS model stood as an independent prognostic factor in pancreatic cancer (Fig. 7B and C). Finally, the IRPS model's predictive capacity for OS was evaluated through ROC curve analysis. The AUC values for 1, 3 and 5 years were 0.657, 0.649 and 0.852, respectively (Fig. 7D). The OS prediction potential of the risk score was further compared against other clinical features at 1 year, yielding the following AUC values: IRPS risk score, 0.657; age, 0.563; gender, 0.548; grade, 0.602; stage, 0.472; T, 0.505; and N, 0.542 (Fig. 7E).

*Relationship between IRPS model and TME*. Recognizing the pivotal role of ICD in response to immunotherapy, an exploration into the association between the IRPS model and the TME was undertaken. The results of this analysis demonstrated a notable association between patients categorized as high-risk

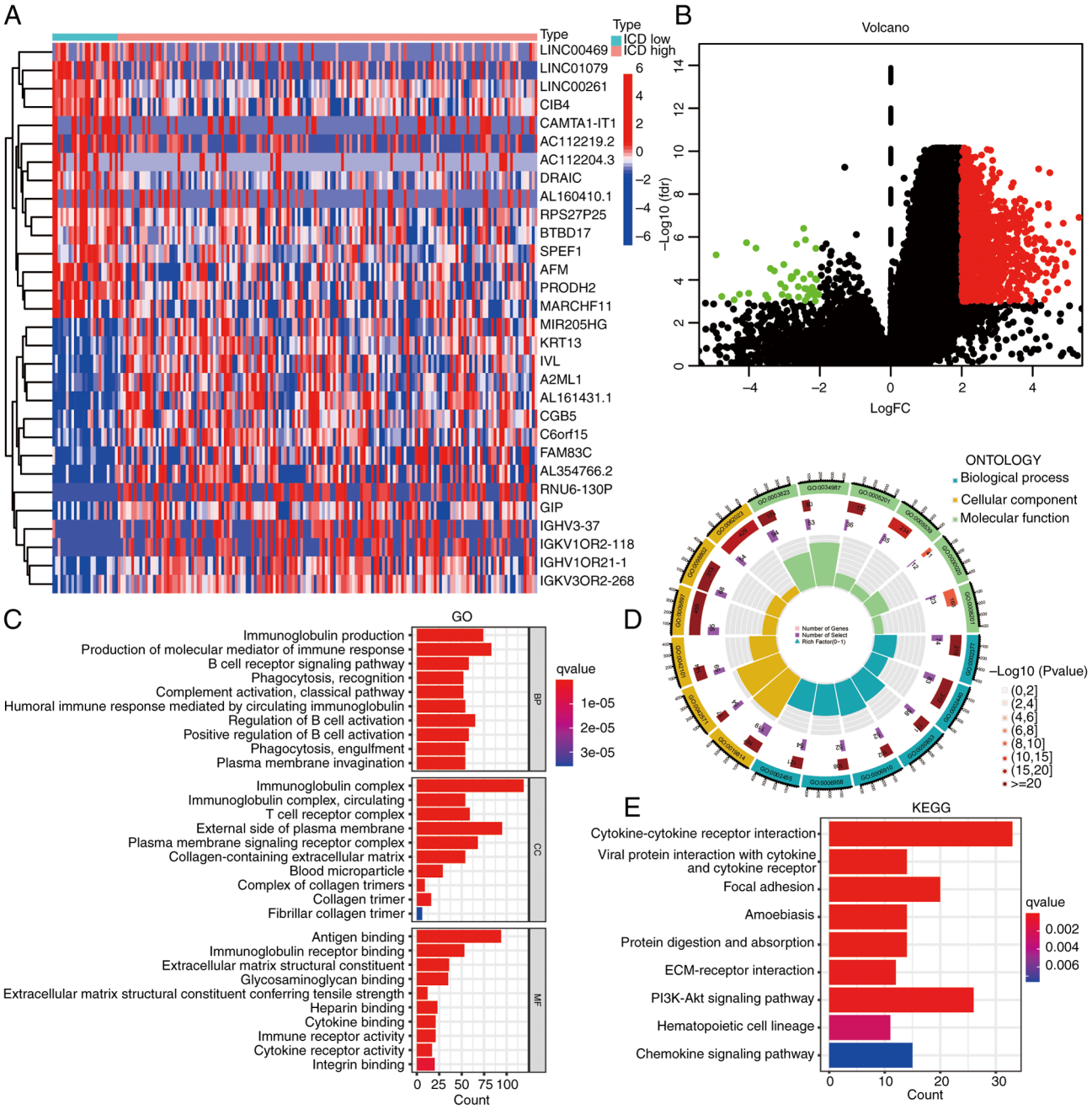


Figure 3. DEGs between the ICD high and ICD low groups. DEGs between ICD high and ICD low group were visualized by (A) a heatmap and (B) volcano plot. (C-E) DEGs were used to perform GO [(C) bubble plot and (D) circle chart] and (E) KEGG (bubble plot) enrichment analyses. ICD, immunogenic cell death; DEGs, differentially expressed genes; FC, fold change; GO, Gene Ontology; KEGG, Kyoto Encyclopedia of Genes and Genomes; BP, Biological Process; CC, Cellular Component; MF, Molecular Function; ECM, extracellular matrix.

and factors such as HLA, T-cell inhibition and checkpoint molecules (Fig. 8A). Furthermore, individuals classified as high-risk were characterized by an elevated frequency of somatic mutations (Fig. 8B and C). Although the TMB score in high-risk patients did not rank extremely high (Fig. 8D), the OS among high-risk patients with an elevated TMB was comparatively shorter compared to other types (Fig. 8E and F). Despite a moderate TIDE score for high-risk patients (Fig. 8G), their OS remained diminished. Further insight revealed that individuals categorized as low-risk exhibited limited sensitivity to 5-Fluorouracil and Gemcitabine treatments (Fig. 9A-D). Of note, these low-risk patients displayed a greater propensity for positive responses to immunotherapy (Fig. 9E). Remarkably, CASP1 and NT5E were also identified as upregulated in pancreatic cancer tissues (Fig. 9F and G). These findings collectively underscore the intricate interplay between the IRPS model, TME, therapeutic responses and the expression of key genes within pancreatic cancer.

*NT5E promotes progression of pancreatic cancer.* Given that CASP1 is a member of the caspase family, its role in tumors has been explored. However, in comparison to NT5E, its significance in research is relatively lower. NT5E has a comprehensive role in the initiation and progression of diverse tumors, exhibiting

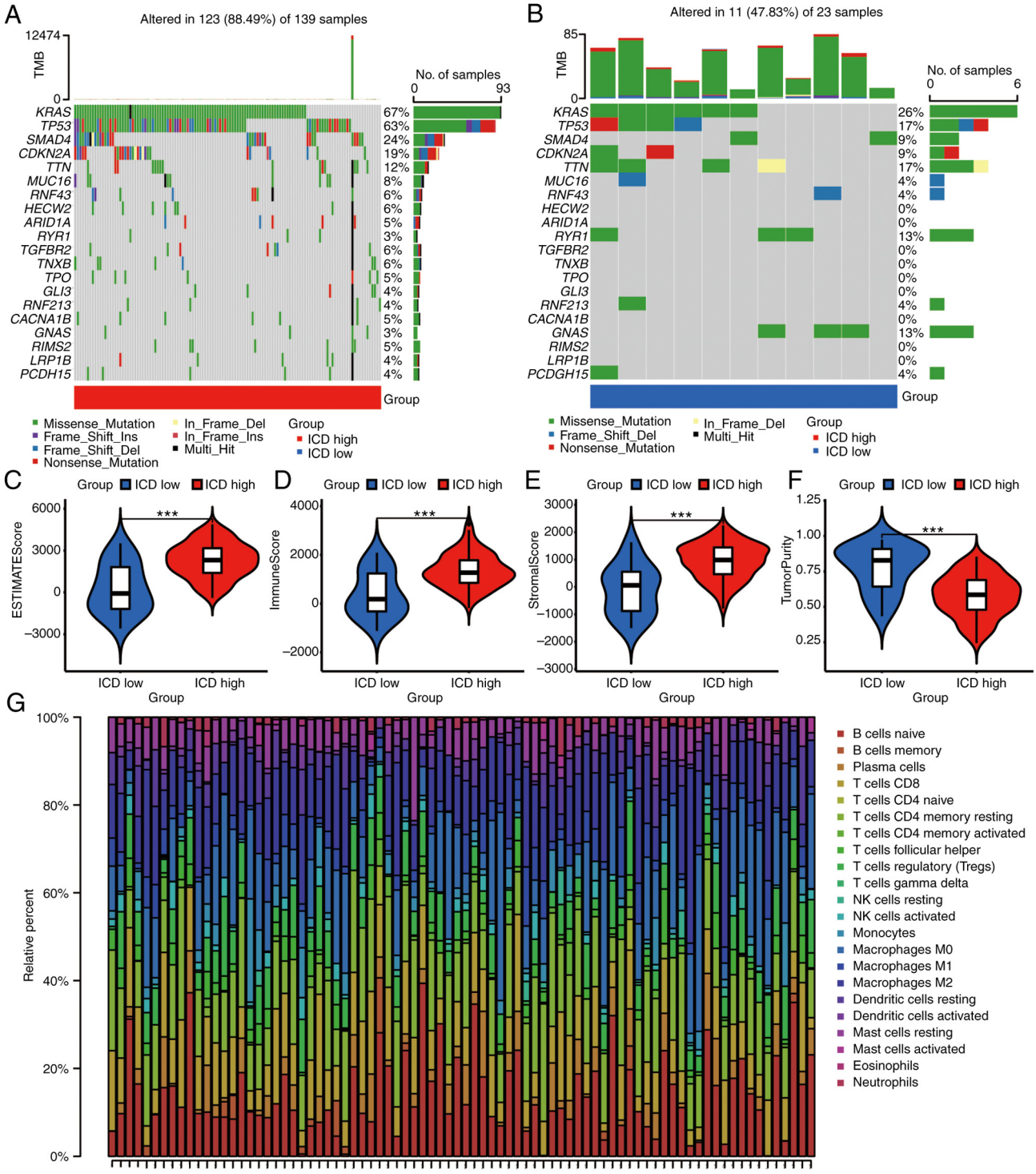


Figure 4. Association between ICD-related genes and tumor microenvironment. The tumor mutation frequency in patients with (A) ICD high was higher than that in patients with (B) ICD low. (C-F) Patients with ICD high had (C) a higher ESTIMATE score, (D) immune score and (E) stromal score and (F) lower tumor purity. (G) Content of immune cells in each pancreatic cancer sample. ***P<0.001. ICD, immunogenic cell death; Del, deletion; Ins, insertion; NK, natural killer; TMB, tumor mutation burden.

intricate and multifaceted mechanisms. This complexity renders it immensely valuable for further investigation. Thus, our focus has shifted to developing a cell line in which NT5E expression is suppressed, allowing us to conduct in-depth functional validation. Finally, the biological function of NT5E was also investigated. Given the observed upregulation of NT5E in pancreatic cancer cells (Fig. 10A and B), lentivirus-mediated knockdown was employed to attenuate NT5E expression in PANC-1 cells (Fig. 10C and D). Seeking to examine the utility of NT5E in the treatment of pancreatic cancer, the effects of downregulated NT5E in conjunction with gemcitabine treatment on pancreatic cancer cells were explored. Of note, the results indicated that the combination of NT5E downregulation and gemcitabine treatment significantly promoted cell apoptosis (Fig. 10E and F). Furthermore, this treatment led to the downregulation of Bcl-2 and upregulation of Bax *in vitro* (Fig. 10G and H). These results

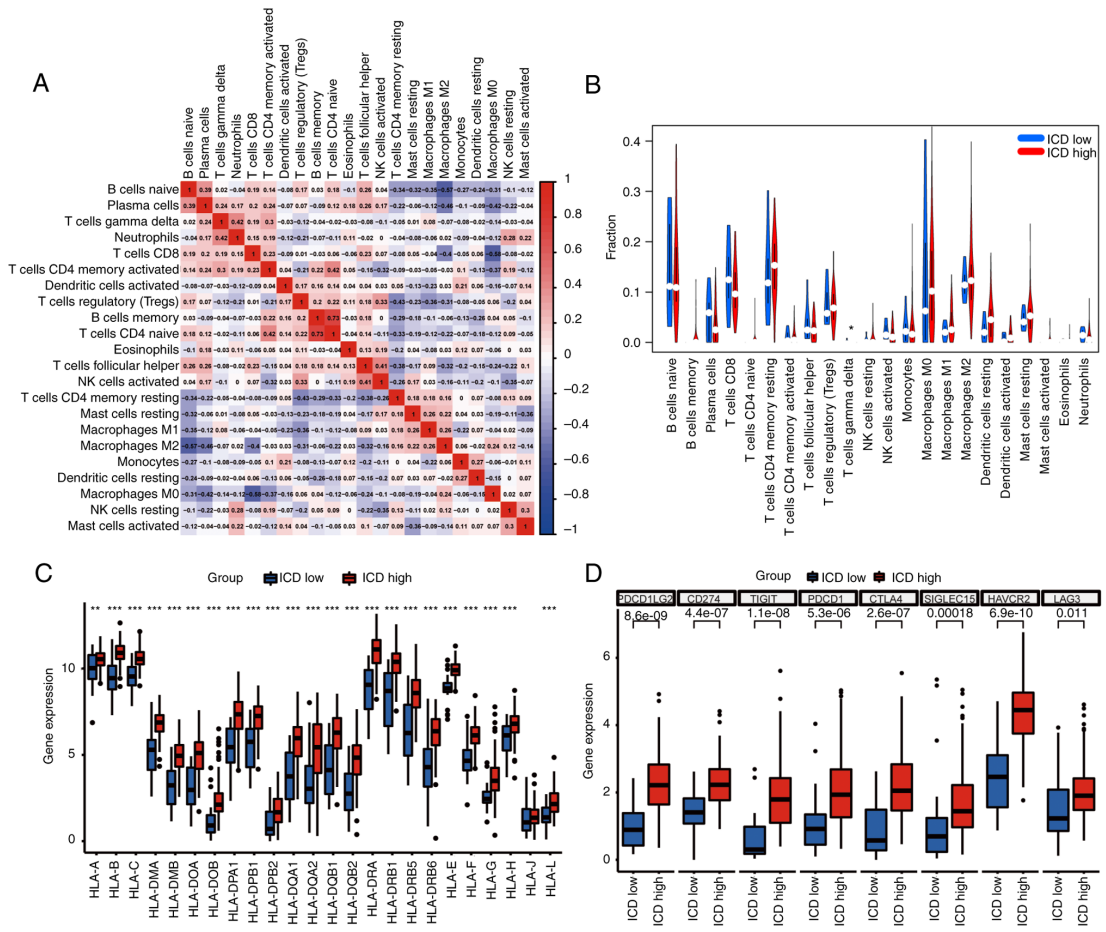


Figure 5. Patients with upregulated ICD-related genes have poor immune status. (A) Correlation between immune cells in each pancreatic cancer sample. (B) The content of T cells gamma delta was upregulated in patients with ICD-high subtype. (C-D) The expression of (C) HLA families or (D) immune checkpoint molecules was upregulated in patients with ICD-high subtype. $^{*}$P<0.05, $^{**}$P<0.01, $^{***}$P<0.001. ICD, immunogenic cell death; NK, natural killer.

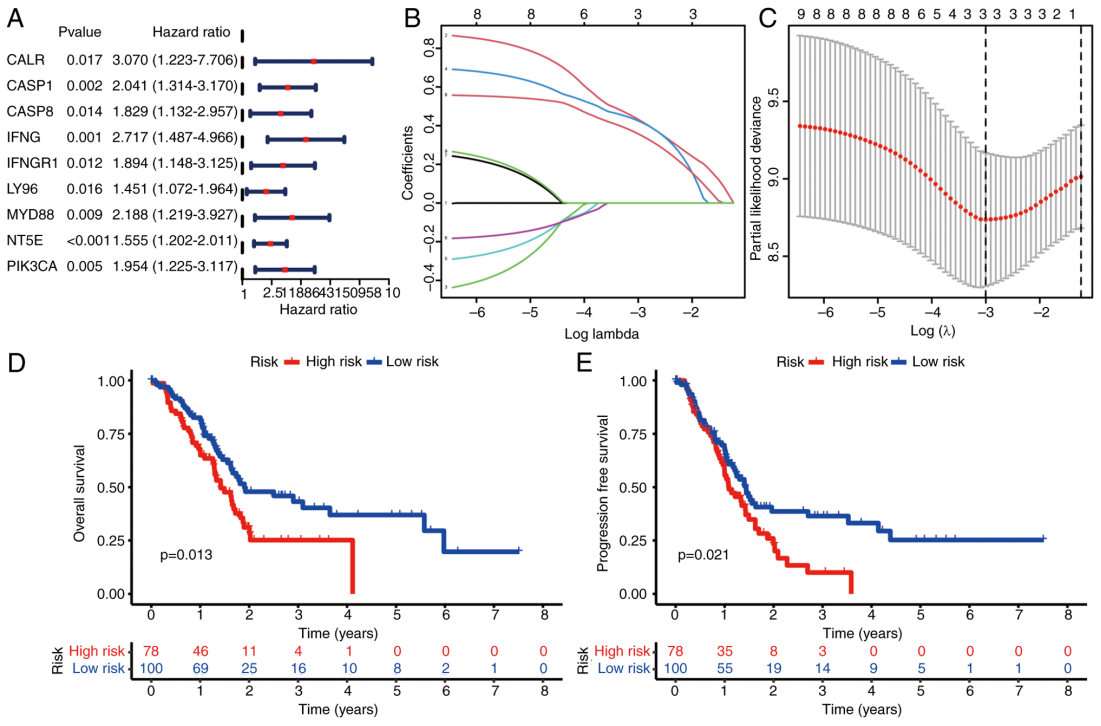


Figure 6. Construction of IRPS in pancreatic cancer. (A) Univariate Cox regression was used to identify 9 prognostic ICD-related genes. (B) Plots of the 10-fold cross-validation error rates. (C) LASSO coefficient profiles of the two ICD-related genes. (D) Overall survival and (E) progression-free survival in patients with a high-risk or low-risk IRPS. IRPS, ICD-related prognostic signature; ICD, immunogenic cell death.

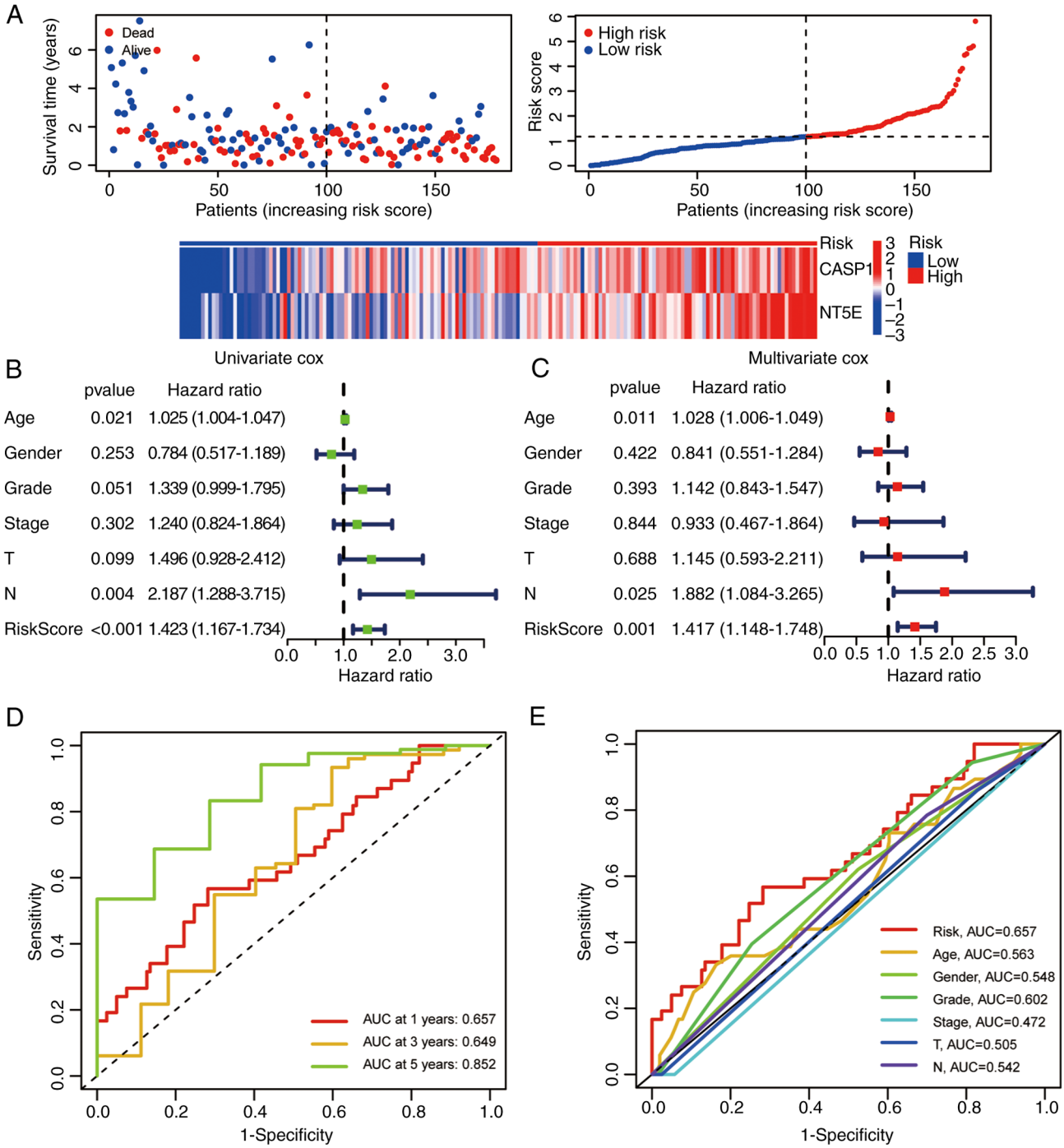


Figure 7. IRPS is an independent prognostic factor in pancreatic cancer. (A) Patients with a high-risk IRPS were more likely to have dead status. (B) Univariate and (C) multivariate Cox regression were used to identify IRPS as an independent prognostic factor. (D) The risk score of IRPS was used to predict survival of patients with pancreatic cancer (1 year: AUC=0.657; 3 years: AUC=0.649; 5 years: AUC=0.852). (E) IRPS risk score and other clinical features were used to predict survival of patients with pancreatic cancer. IRPS, immunogenic cell death-related prognostic signature; AUC, area under the curve.

collectively underscore the potential role of NT5E in influencing pancreatic cancer cell responses to treatment, particularly in combination with gemcitabine.

## Discussion

Recent research has accumulated a wealth of evidence underscoring the pivotal role played by the tumor immune microenvironment in the evolution of pancreatic cancer (13,14). Despite numerous clinical trials aimed at evaluating the effectiveness of diverse immunotherapeutic strategies in managing pancreatic cancer, such as ICIs, cancer vaccines and chemotherapy, the outcomes from a majority of these trials have been underwhelming (15-17). Of note, the quest to identify reliable biomarkers capable of categorizing patients based on their responsiveness to immunotherapy (18), particularly ICD immunotherapy, has emerged as a significant pursuit. In the present study, the segmentation of pancreatic cancer samples into two distinctive subtypes was achieved through the application of ICD-related genes. These findings demonstrated the

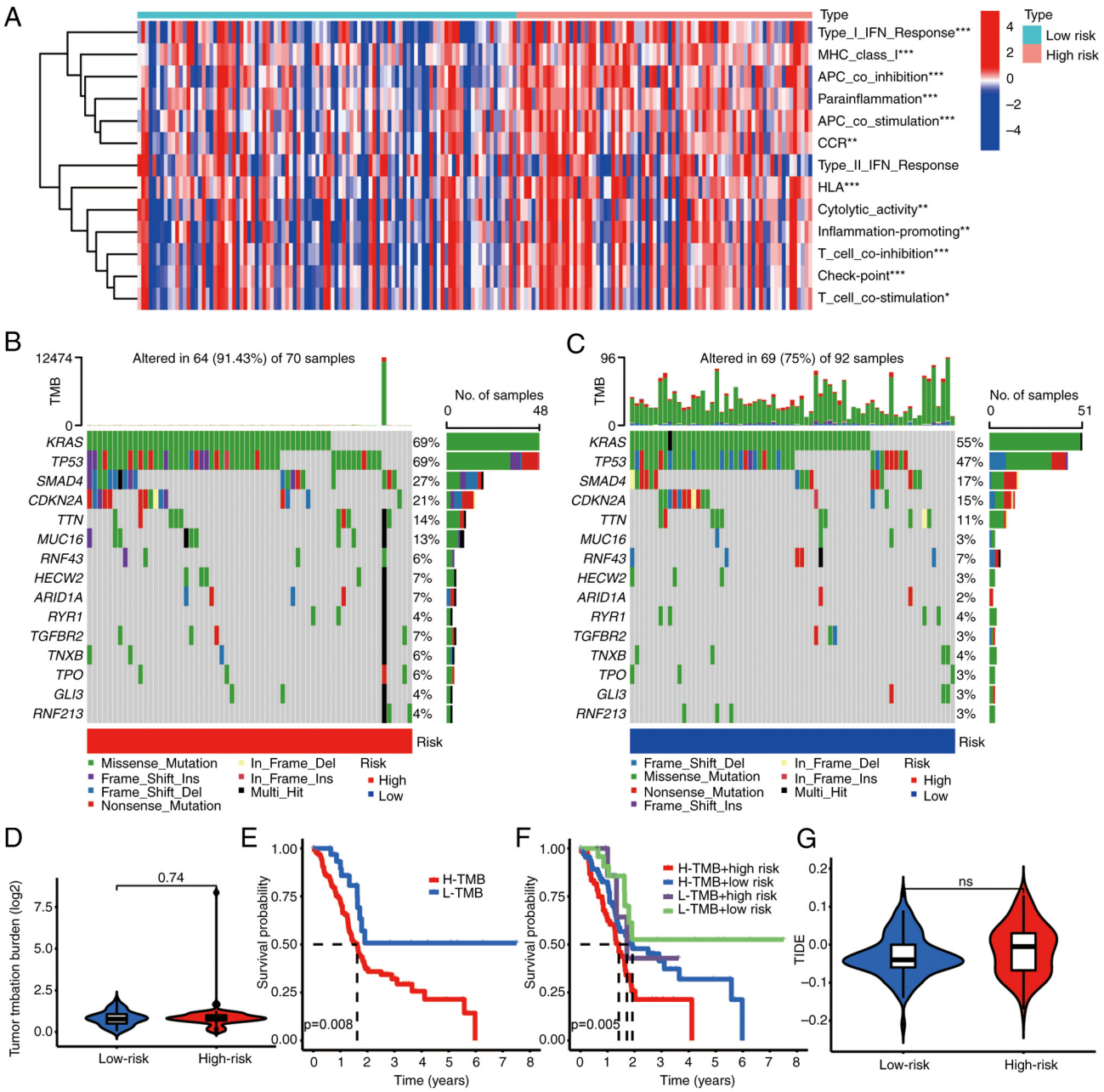


Figure 8. Association between IRPS and tumor mutation. (A) Patients with a high-risk IRPS were correlated with immune function (type I IFN response, MHC class I, APC co-inhibition, etc.). (B and C) Patients with (B) a high-risk IRPS had a higher mutation frequency than (C) those with a low-risk IRPS. (D) The TMB score in the high-risk group exhibited a trend to be higher. (E) Patients with a high TMB score had poor prognosis. (F) Patients with a high-risk IRPS had poor prognosis. (G) Association between IRPS risk score and TIDE score. $^{*}$P<0.05, $^{**}$P<0.01, $^{***}$P<0.001. IRPS, immunogenic cell death-related prognostic signature; Del, deletion; Ins, insertion; ns, no significance; APC, antigen-presenting cell; IFN, interferon; H/L-TMB, high/low tumor mutation burden; TIDE, Tumor Immune Dysfunction and Exclusion; TMB, tumor mutation burden.

potential of ICD-related genes to provide a benefit for patients undergoing chemotherapy or immunotherapy.

The present study revealed that patients classified under the ICD high subtype exhibited a compromised immune status and prognosis. During the process of ICD induction, deteriorating tumor cells release DAMPs. Subsequent to ICD, these DAMPs activate pattern recognition receptors present on macrophages, dendritic cells and natural killer cells, thereby triggering T-cell activation and the initiation of immune responses (19). Furthermore, the utilization of ICIs was observed to bolster the activity of effector T cells, subsequently augmenting the anti-tumor efficacy (20). In line with these findings, the present results demonstrated that the DEGs were closely linked to immune function. Of note, the expression of genes belonging to the HLA families and checkpoint molecules was markedly upregulated in patients from the ICD-high group. These results strongly suggest the potential of ICD-related genes to have a role in enhancing the effectiveness of ICI treatment for patients with pancreatic cancer.

Moving forward, the present study unveiled a noteworthy trend: Patients characterized by a high IRPS risk score exhibited a higher likelihood of responding positively to chemotherapy or immunotherapy within the context of pancreatic cancer treatment. The TME in pancreatic cancer

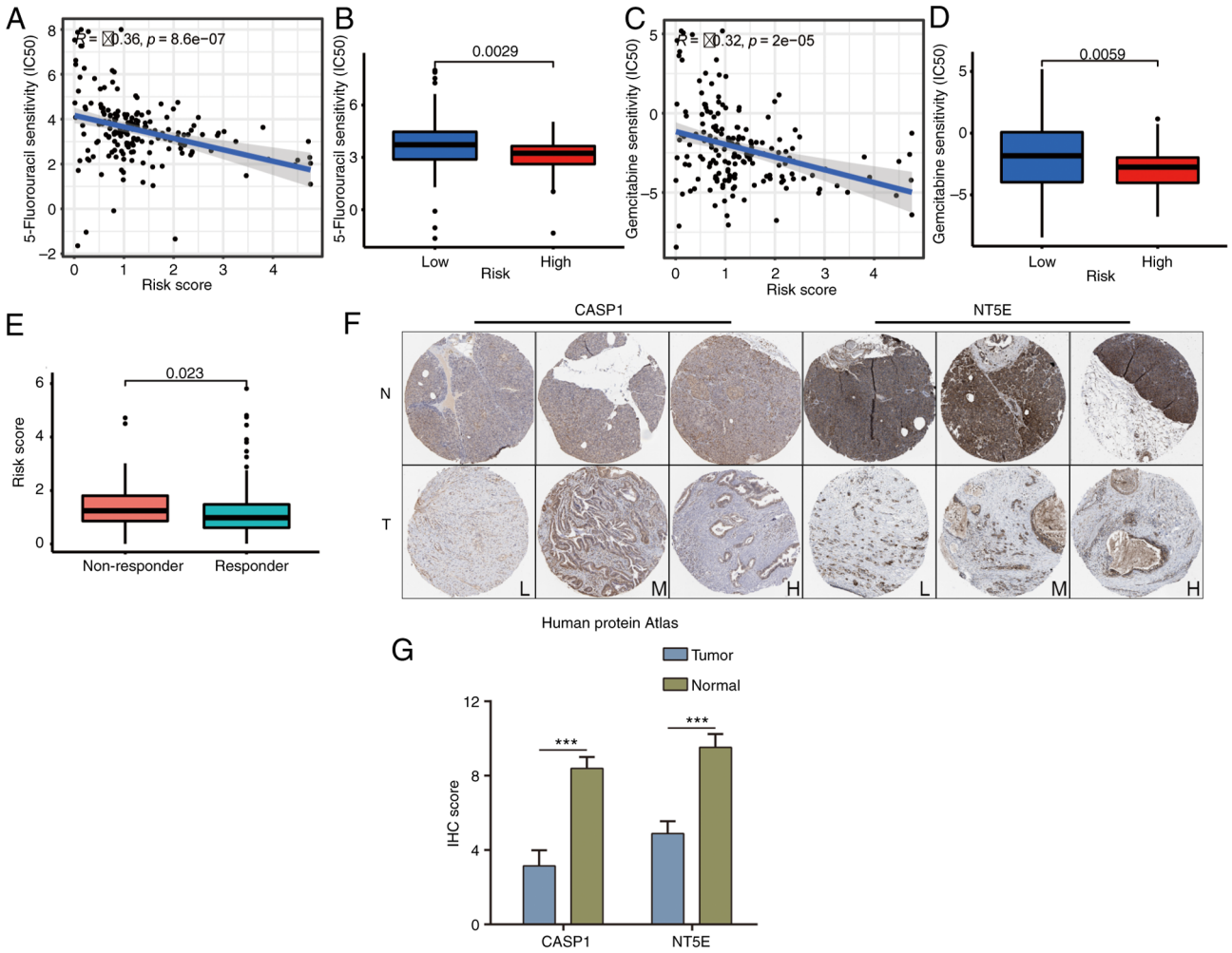


Figure 9. IRPS was used to predict drug sensitivity and response to immunotherapy. (A) The IRPS score was negatively correlated with the $IC_{50}$ of 5-Fluorouracil. (B) The $IC_{50}$ of 5-Fluorouracil was lower in the high-risk IRPS group. (C) The IRPS score was negatively correlated with the $IC_{50}$ of Gemcitabine. (D) The $IC_{50}$ of Gemcitabine was lower in the high-risk IRPS group. (E) Patients with a high-risk IRPS were not responsive to immunotherapy. (F) Expression of CASP1 and NT5E in pancreatic cancer tissues from The Human Protein Atlas. (G) Quantified IHC score of CASP1 and NT5E in The Human Protein Atlas samples. ***P<0.01. L, poor differentiation; M, moderate differentiation; H, high differentiation; T, tumor sample; N, normal sample; NT5E, 5'-nucleotidase ecto; CASP1, caspase 1; IRPS, immunogenic cell death-related prognostic signature; IHC, immunohistochemistry.

comprises a diverse array of immune cells with varying functions. Among these are CD4+/CD8+ T cells, natural killer cells and dendritic cells, all of which exert anti-tumor effects. Conversely, the TME is abundant in immunosuppressive elements, such as regulatory T cells, myeloid-derived suppressor cells and tumor-associated macrophages (21). These cells secrete an array of immunosuppressive factors, including IL-10, IL-23, TGF-β and indoleamine 2,3-dioxygenase 1, contributing to the formation of an immunosuppressive milieu conducive to pancreatic cancer progression (22-24). Consequently, this immunosuppressive TME curtails the immune response, leading to immune evasion and thereby influencing the efficacy of immunotherapeutic approaches in treating pancreatic cancer. In light of these observations, it becomes apparent that the IRPS model, in conjunction with ICIs, holds promise as an effective strategy to enhance the outcomes of immunotherapy for pancreatic cancer.

Furthermore, it is worth highlighting that both NT5E and CASP1, key components in the construction of the IRPS model, were upregulated in pancreatic cancer tissues. In line with this, Angelova *et al* (25) reported that the infection of pancreatic cancer cells by oncolytic parvovirus H-1 triggers signaling via the secretion of the alarmin HMGB1 and activation of an inflammasome/CASP1 platform. Of note, the CASP1/4/5 genes have a role in regulating innate immunity and T-cell responses, suggesting their potential to enhance tumor checkpoint inhibition (26). While CASP1's role as part of the caspase family has prompted scrutiny, its significance as a downstream factor within the apoptotic pathway has somewhat dampened its research appeal, particularly when compared to the multifaceted and prominent NT5E. The intricate involvement of NT5E across diverse aspects of tumor initiation and progression enhances its research relevance substantially. Consequently, our focus remains on establishing a cell line characterized by suppressed NT5E expression for rigorous functional validation. Importantly, previous investigations have hinted at NT5E's involvement in inducing resistance to gemcitabine. Thus, our strategy involves combining targeted intervention against NT5E with gemcitabine treatment, aiming to determine whether NT5E targeting may

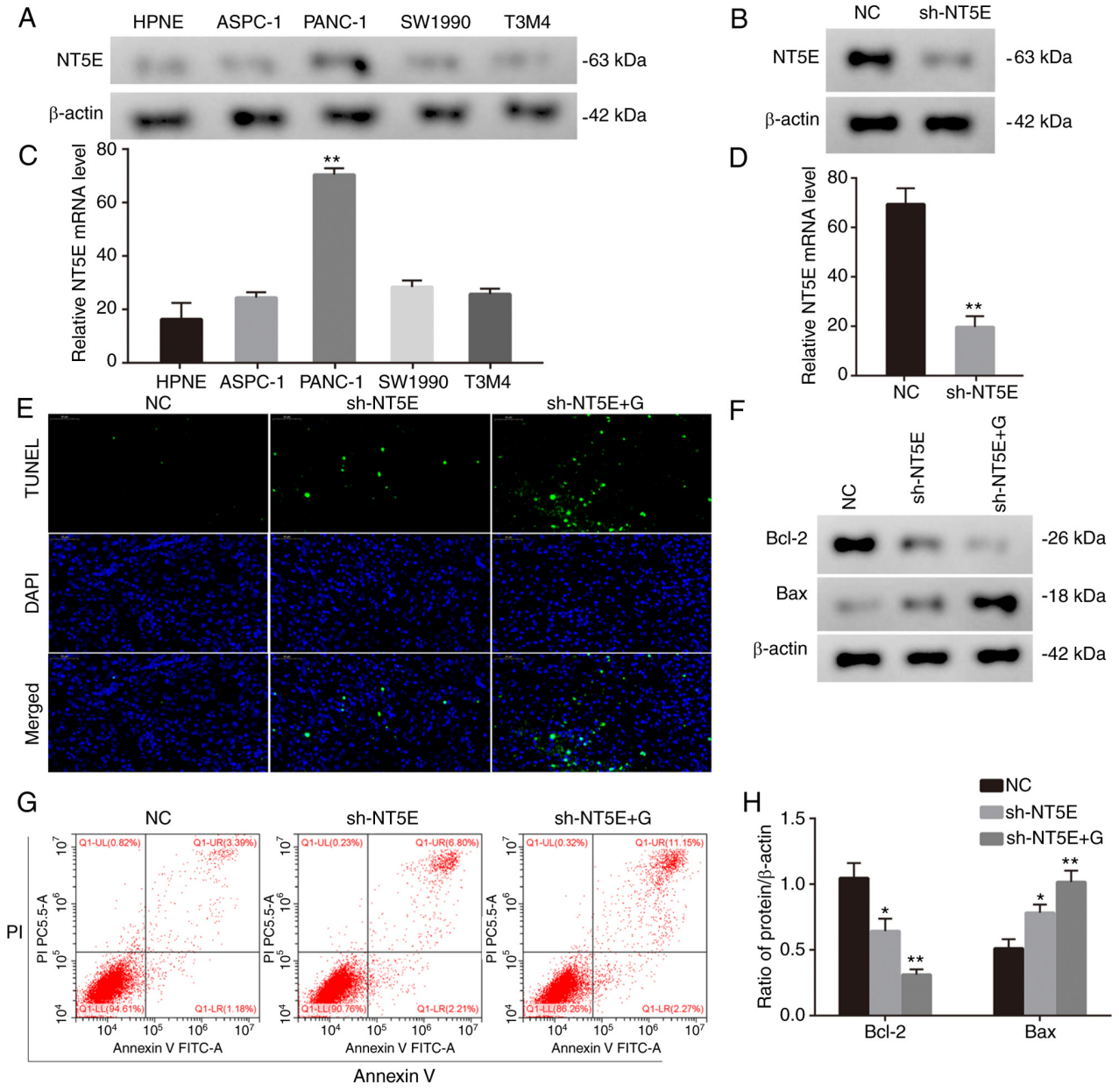


Figure 10. Biological function of NT5E. (A and B) NT5E was upregulated in PANC-1 cells. (A) Western blotting bands and (B) quantitative results. (C and D) Lentivirus was used to downregulate NT5E in PANC-1 cells. (C) Western blot bands and (D) quantitative results indicating successful knockdown of NT5E. (E and F) Downregulation of NT5E combined with gemcitabine treatment promoted PANC-1 cell apoptosis. (E) Fluorescence microscopy images of TUNEL stain (magnification, x400) and (F) flow cytometry dot plots of Annexin V/PI double staining. (G and H) Downregulation of NT5E combined with gemcitabine treatment regulated apoptosis-related proteins. (G) Western blotting bands and (H) quantitative results. $^{*}$P<0.05, $^{**}$P<0.01 vs. NC; Images are representative of at least three independent experiments. Values are expressed as the mean ± standard error of the mean. NC, negative control; G, Gemcitabine; NT5E, 5'-nucleotidase ecto; NC, negative control; sh-NT5E, short hairpin RNA targeting NT5E; PI, propidium iodide.

potentially counteract gemcitabine resistance within pancreatic cancer scenarios. Furthermore, the present study revealed that NT5E displayed upregulation in the pancreatic cell line PANC-1 and patients with a lower IRPS risk score exhibited increased sensitivity to 5-Fluorouracil and Gemcitabine. Intriguingly, the combination of NT5E downregulation and Gemcitabine treatment was found to facilitate cell apoptosis. These findings are in accordance with the observations made by Chen *et al* (27), who proposed a correlation between higher NT5E expression and elevated programmed death-ligand 1 expression and TMB in patients with pancreatic cancer. In addition, King *et al* (28) noted an increase in IFN-γ expression by intratumoral CD4+ and CD8+ cells upon NT5E knockdown in pancreatic cancer. In light of these findings, inhibition of NT5E in conjunction with Gemcitabine holds promise as a potentially impactful therapeutic approach for pancreatic cancer.

However, it is important to acknowledge that the current study is not without its limitations. First, the scarcity of available GEO datasets pertaining to pancreatic cancer posed challenges in the external validation of the IRPS model. Furthermore, the relatively limited sample size within the TCGA pancreatic cancer dataset may potentially compromise the statistical robustness of the findings. Finally, it becomes evident that further experimentation is required to substantiate the underlying molecular

mechanisms associated with NT5E in the context of pancreatic cancer. In future research, *in vivo* and *in vitro* experiments will be designed to validate the functions of NT5E. In addition, RNA sequencing should be conducted to identify the pathways and functions influenced by it.

In conclusion, the present study has provided valuable insight into the intricate interplay between ICD clusters and the tumor immune microenvironment within the realm of pancreatic cancer. Furthermore, an IRPS model that holds the capability to predict OS and the potential response to immunotherapy among individuals with pancreatic cancer was successfully developed.

**Acknowledgements**

Not applicable.

**Funding**

No funding was received.

**Availability of data and materials**

The datasets used and/or analyzed during the current study are available from the corresponding author on reasonable request.

**Authors' contributions**

JX was responsible for conceptualization, ML for data collection and analysis, and supervision, and WY for the formal analysis. WY and JX helped review and edit the manuscript. JZ, ML and WY confirm the authenticity of all the raw data. All authors have read and approved the final version of the manuscript.

**Ethics approval and consent to participate**

Not applicable.

**Patient consent for publication**

Not applicable.

**Declaration of interest**

The authors declare that they have no competing interests.

**References**

1. Versteijne E, van Dam JL, Suker M, Janssen QP, Groothuis K, Akkermans-Vogelaar JM, Besselink MG, Bonsing BA, Buijsen J, Busch OR, *et al*: Neoadjuvant chemoradiotherapy versus upfront surgery for resectable and borderline resectable pancreatic cancer: Long-term results of the Dutch randomized PREOPANC trial. J Clin Oncol 40: 1220-1230, 2022.
2. Truty MJ, Kendrick ML, Nagorney DM, Smoot RL, Cleary SP, Graham RP, Goenka AH, Hallemeier CL, Haddock MG, Harmsen WS, *et al*: Factors predicting response, perioperative outcomes, and survival following total neoadjuvant therapy for borderline/locally advanced pancreatic cancer. Ann Surg 273: 341-349, 2021.
3. Wu J and Cai J: Dilemma and challenge of immunotherapy for pancreatic cancer. Dig Dis Sci 66: 359-368, 2021.
4. Zong L, Mo S, Sun Z, Lu Z, Yu S, Chen J and Xiang Y: Analysis of the immune checkpoint V-domain Ig-containing suppressor of T-cell activation (VISTA) in endometrial cancer. Mod Pathol 35: 266-273, 2022.
5. Ortega MA, Fraile-Martinez O, Pekarek L, Garcia-Montero C, Alvarez-Mon MA, Castellanos AJ, García-Honduvilla N, Buján J, Alvarez-Mon M, Sáez MA, *et al*: Oxidative stress markers are associated with a poor prognosis in patients with pancreatic cancer. Antioxidants (Basel) 11: 759, 2022.
6. Fucikova J, Kepp O, Kasikova L, Petroni G, Yamazaki T, Liu P, Zhao L, Spisek R, Kroemer G and Galluzzi L: Detection of immunogenic cell death and its relevance for cancer therapy. Cell Death Dis 11: 1013, 2020.
7. Kim R and Kin T: Current and future therapies for immunogenic cell death and related molecules to potentially cure primary breast cancer. Cancers (Basel) 13: 4756, 2021.
8. Hayashi K, Nikolos F and Chan KS: Inhibitory DAMPs in immunogenic cell death and its clinical implications. Cell Stress 5: 52-54, 2021.
9. Yang S, Tang W, Azizian A, Gaedcke J, Ströbel P, Wang L, Cawley H, Ohara Y, Valenzuela P, Zhang L, *et al*: Dysregulation of HNF1B/Clusterin axis enhances disease progression in a highly aggressive subset of pancreatic cancer patients. Carcinogenesis 43: 1198-1210, 2022.
10. Wang X, Wu S, Liu F, Ke D, Wang X, Pan D, Xu W, Zhou L and He W: An immunogenic cell death-related classification predicts prognosis and response to immunotherapy in head and neck squamous cell carcinoma. Front Immunol 12: 781466, 2021.
11. Garg AD, De Ruysscher D and Agostinis P: Immunological metagene signatures derived from immunogenic cancer cell death associate with improved survival of patients with lung, breast or ovarian malignancies: A large-scale meta-analysis. Oncoimmunology 5: e1069938, 2015.
12. Ahn HR, Baek GO, Yoon MG, Son JA, You D, Yoon JH, Cho HJ, Kim SS, Cheong JY and Eun JW: HMBS is the most suitable reference gene for RT-qPCR in human HCC tissues and blood samples. Oncol Lett 22: 791, 2021.
13. Grünwald BT, Devisme A, Andrieux G, Vyas F, Aliar K, McCloskey CW, Macklin A, Jang GH, Denroche R, Romero JM, *et al*: Spatially confined sub-tumor microenvironments in pancreatic cancer. Cell 184: 5577-5592.e18, 2021.
14. Pekarek L, Fraile-Martinez O, Garcia-Montero C, Alvarez-Mon MA, Acero J, Ruiz-Llorente L, García-Honduvilla N, Albillos A, Buján J, Alvarez-Mon M, *et al*: Towards an updated view on the clinical management of pancreatic adenocarcinoma: Current and future perspectives. Oncol Lett 22: 809, 2021.
15. Fan JQ, Wang MF, Chen HL, Shang D, Das JK and Song J: Current advances and outlooks in immunotherapy for pancreatic ductal adenocarcinoma. Mol Cancer 19: 32, 2020.
16. Reiss KA, Mick R, O'Hara MH, Teitelbaum U, Karasic TB, Schneider C, Cowden S, Southwell T, Romeo J, Izgur N, *et al*: Phase II study of maintenance rucaparib in patients with platinum-sensitive advanced pancreatic cancer and a pathogenic germline or somatic variant in BRCA1, BRCA2, or PALB2. J Clin Oncol 39: 2497-2505, 2021.
17. Parikh AR, Szabolcs A, Allen JN, Clark JW, Wo JY, Raabe M, Thel H, Hoyos D, Mehta A, Arshad S, *et al*: Radiation therapy enhances immunotherapy response in microsatellite stable colorectal and pancreatic adenocarcinoma in a phase II trial. Nat Cancer 2: 1124-1135, 2021.
18. Pekarek L, Fraile-Martinez O, Garcia-Montero C, Saez MA, Barquero-Pozanco I, Del Hierro-Marlasca L, de Castro Martinez P, Romero-Bazán A, Alvarez-Mon MA, Monserrat J, *et al*: Clinical applications of classical and novel biological markers of pancreatic cancer. Cancers (Basel) 14: 1866, 2022.
19. Jentho E and Weis S: DAMPs and innate immune training. Front Immunol 12: 699563, 2021.
20. Jardim DL, Goodman A, de Melo Gagliato D and Kurzrock R: The challenges of tumor mutational burden as an immunotherapy biomarker. Cancer Cell 39: 154-173, 2021.
21. Liu YT and Sun ZJ: Turning cold tumors into hot tumors by improving T-cell infiltration. Theranostics 11: 5365-5386, 2021.
22. Zhang X, Lao M, Xu J, Duan Y, Yang H, Li M, Ying H, He L, Sun K, Guo C, *et al*: Combination cancer immunotherapy targeting TNFR2 and PD-1/PD-L1 signaling reduces immunosuppressive effects in the microenvironment of pancreatic tumors. J Immunother Cancer 10: e003982, 2022.
23. Wang X, Wang L, Mo Q, Dong Y, Wang G and Ji A: Changes of Th17/Treg cell and related cytokines in pancreatic cancer patients. Int J Clin Exp Pathol 8: 5702-5708, 2015.

24. Gabitova-Cornell L, Surumbayeva A, Peri S, Franco-Barraza J, Restifo D, Weitz N, Ogier C, Goldman AR, Hartman TR, Francescone R, *et al*: Cholesterol pathway inhibition induces TGF-β signaling to promote basal differentiation in pancreatic cancer. Cancer Cell 38: 567-583.e11, 2020.
25. Angelova AL, Grekova SP, Heller A, Kuhlmann O, Soyka E, Giese T, Aprahamian M, Bour G, Rüffer S, Cziepluch C, *et al*: Complementary induction of immunogenic cell death by oncolytic parvovirus H-1PV and gemcitabine in pancreatic cancer. J Virol 88: 5263-5276, 2014.
26. Hong W, Gu Y, Guan R, Xie D, Zhou H and Yu M: Pan-cancer analysis of the CASP gene family in relation to survival, tumor-infiltrating immune cells and therapeutic targets. Genomics 112: 4304-4315, 2020.
27. Chen Q, Pu N, Yin H, Zhang J, Zhao G, Lou W and Wu W: CD73 acts as a prognostic biomarker and promotes progression and immune escape in pancreatic cancer. J Cell Mol Med 24: 8674-8686, 2020.
28. King RJ, Shukla SK, He C, Vernucci E, Thakur R, Attri KS, Dasgupta A, Chaika NV, Mulder SE, Abrego J, *et al*: CD73 induces GM-CSF/MDSC-mediated suppression of T cells to accelerate pancreatic cancer pathogenesis. Oncogene 41: 971-982, 2022.